IL NUOVO CIMENTO **38 C** (2015) 132
DOI 10.1393/ncc/i2015-15132-0

COLLOQUIA: LaThuile15

NA48/2 studies of rare decays

M. RAGGI for the NA48/2 COLLABORATION(*)
INFN, Laboratori Nazionali di Frascati - via E. Fermi 40, Frascati, Italy

received 2 October 2015

Summary. — The first observation of about 2000 candidates, with a background contamination below 3%, of the rare decay $K^\pm \to \pi^\pm\pi^0 e^+ e^-$ is reported by the NA48/2 experiment. The preliminary branching ratio in the full kinematic region is obtained to be: $\mathcal{B}(K^\pm \to \pi^\pm\pi^0 e^+ e^-) = (4.06 \pm 0.17) \cdot 10^{-6}$ by analyzing the data collected in 2003. A sample of 4.687×10^6 $K^\pm \to \pi^\pm\pi^0_D$, decay candidates with a negligible background contamination collected in 2003–04 is analyzed to search for the dark photon (A') via the decay chain $K^\pm \to \pi^\pm\pi^0$, $\pi^0 \to \gamma A'$, $A' \to e^+e^-$. No signal is observed, and preliminary limits in the plane dark photon mixing parameter ε^2 *vs.* its mass $m_{A'}$ are reported.

1. – The NA48/2 experiment

The NA48/2 experiment at the CERN SPS collected a large sample of charged kaon ($K^\pm$) decays during its 2003–04 data taking period. The NA48/2 beam line has been

(*) NA48/2 Collaboration: G. Anzivino, R. Arcidiacono, W. Baldini, S. Balev, J. R. Batley, M. Behler, S. Bifani, C. Biino, A. Bizzeti, B. Bloch-Devaux, G. Bocquet, N. Cabibbo, M. Calvetti, N. Cartiglia, A. Ceccucci, P. Cenci, C. Cerri, C. Cheshkov, J. B. Chèze, M. Clemencic, G. Collazuol, F. Costantini, A. Cotta Ramusino, D. Coward, D. Cundy, A. Dabrowski, P. Dalpiaz, C. Damiani, M. De Beer, J. Derré, H. Dibon, L. DiLella, N. Doble, K. Eppard, V. Falaleev, R. Fantechi, M. Fidecaro, L. Fiorini, M. Fiorini, T. Fonseca Martin, P. L. Frabetti, L. Gatignon, E. Gersabeck, A. Gianoli, S. Giudici, A. Gonidec, E. Goudzovski, S. Goy Lopez, M. Holder, P. Hristov, E. Iacopini, E. Imbergamo, M. Jeitler, G. Kalmus, V. Kekelidze, K. Kleinknecht, V. Kozhuharov, W. Kubischta, G. Lamanna, C. Lazzeroni, M. Lenti, L. Litov, D. Madigozhin, A. Maier, I. Mannelli, F. Marchetto, G. Marel, M. Markytan, P. Marouelli, M. Martini, L. Masetti, E. Mazzucato, A. Michetti, I. Mikulec, N. Molokanova, E. Monnier, U. Moosbrugger, C. Morales Morales, D. J. Munday, A. Nappi, G. Neuhofer, A. Norton, M. Patel, M. Pepe, A. Peters, F. Petrucci, M. C. Petrucci, B. Peyaud, M. Piccini, G. Pierazzini, I. Polenkevich, Yu. Potrebenikov, M. Raggi, B. Renk, P. Rubin, G. Ruggiero, M. Savrié, M. Scarpa, M. Shieh, M. W. Slater, M. Sozzi, S. Stoynev, E. Swallow, M. Szleper, M. Valdata-Nappi, B. Vallage, M. Velasco, M. Veltri, S. Venditti, M. Wache, H. Wahl, A. Walker, R. Wanke, L. Widhalm, A. Winhart, R. Winston, M. D. Wood, S. A. Wotton, A. Zinchenko, M. Ziolkowski.

designed to deliver simultaneous narrow momentum band K^+ and K^- beams originating from the collision of the primary 400 GeV/c protons extracted from the CERN SPS on a beryllium target. Secondary beams with central momenta of (60 ± 3) GeV/c (r.m.s.) following a common beam axis were used. The beam kaons decayed in a fiducial decay volume contained in a 114 m long cylindrical vacuum tank. The momenta of charged decay products were measured in a magnetic spectrometer, housed in a tank filled with helium placed after the decay volume. The spectrometer comprised four drift chambers (DCHs) and a dipole magnet. A plastic scintillator hodoscope (CHOD) producing fast trigger signals and providing precise time measurements of charged particles was placed after the spectrometer. Further downstream was a liquid krypton electromagnetic calorimeter (LKr), an almost homogeneous ionization chamber with an active volume of 7 m^3 of liquid krypton, $27X_0$ deep, segmented transversally into 13248 projective $\sim 2\times 2$ cm^2 cells and with no longitudinal segmentation. An iron/scintillator hadronic calorimeter and muon detectors were located further downstream. A dedicated two-level trigger was used to collect three track decays with a very high efficiency. A detailed description of the detector can be found in [1].

2. – First observation of $K^\pm \to \pi^\pm\pi^0 e^+e^-$ decay

The $K^\pm \to \pi^\pm\pi^0 e^+e^-$ decay proceeds through virtual photon exchange which undergoes internal conversion into electron-positron pair, *i.e.* $K^\pm \to \pi^\pm\pi^0\gamma^* \to \pi^\pm\pi^0 e^+e^-$. The γ^* is produced by two different mechanisms: Inner Bremsstrahlung (IB), where the γ^* is emitted by one of the charged mesons in the initial or final state and Direct Emission (DE) when γ^* is radiated off at the weak vertex of the intermediate state. As a consequence the differential decay width consists of three terms: the dominant long-distance IB contribution (pure electric part E), the DE component (electric E and magnetic M parts) and the interference between them [2]. The interference term collects the different contributions, IBE, IBM and EM. For this reason the $\pi^\pm\pi^0 e^+e^-$ decay offers interesting short and long distance parity violating observables. In the $K^\pm \to \pi^\pm\pi^0\gamma$ mode the interference consists only of the IBE term [3], because the remaining (EM) interferences are P-violating, but cancel out upon angular integration. There are few theoretical publications related to the $K^\pm \to \pi^\pm\pi^0 e^+e^-$ [2, 4, 5]. Recently authors of [2] where able to predict, on the basis of the NA48/2 measurement of the magnetic and electric terms in $K^\pm \to \pi^\pm\pi^0\gamma$ [6], the branching ratio of the single components. No experimental observation has so far been reported.

2·1. *Selection and background estimates.* – $K^\pm \to \pi^\pm\pi^0 e^+e^-$ event candidates are reconstructed from three charged tracks and two photons, forming neutral pion, pointing to a common vertex in the fiducial decay volume. Particle identification is based on the energy deposition in LKr (E) associated or not to a charged track momentum (p) measured in the spectrometer. The charged track is identified as electron/positron if its E/p ratio is greater than 0.85, and as a charged pion if the E/p ratio is lower than 0.85. Two isolated energy clusters without associated track in the LKr are identified as the two candidates photons from the π^0 decay. Their invariant mass is required to be within ± 10 MeV/c^2 from the nominal PDG [7] π^0 mass. The reconstructed invariant mass of the $\pi^\pm\pi^0 e^+e^-$ system is required to be within ± 10 MeV/c^2 from the nominal PDG [7] $K^\pm$ mass. Two main sources of background are contribution to the signal final state: $K^\pm \to \pi^\pm\pi^0\pi^0_D$ ($K_{3\pi D}$) when one of the photon is lost, and $K^\pm \to \pi^\pm\pi^0_D(\gamma)$ ($K_{2\pi D}$), where π^0_D denotes the π^0 Dalitz decay $\pi^0 \to e^+e^-\gamma$. The suppression of the

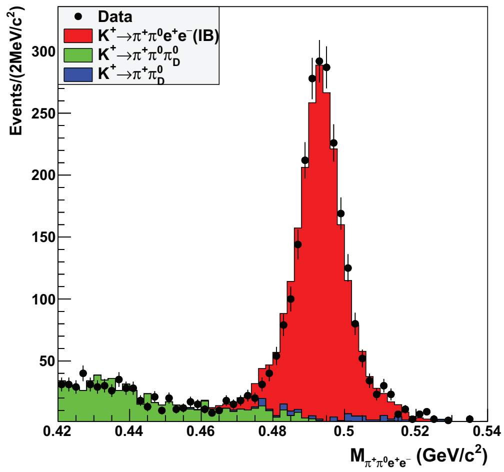

Fig. 1. – Reconstructed $\pi^{\pm}\pi^0 e^+e^-$ invariant mass distributions of the data and simulated background samples.

$K_{3\pi D}$ background events is obtained by requiring the squared invariant mass of the $\pi^+\pi^0$ system to be greater than $120\,\mathrm{MeV}^2/c^4$, exploiting the presence of three particles with almost the same mass in the final state. In order to reject $K_{2\pi D}$ background contamination both the invariant masses $M_{ee\gamma_{1,2}}$ are required to be more than $7\,\mathrm{MeV}/c^2$ away from the nominal mass of the neutral pion. Analyzing the 2003 data, a sample of 1916 signal candidates has been selected with a background contamination below 3%. In particular MC simulation predicts a contribution of (26 ± 5.1) candidates form $K_{2\pi D}$ and (30 ± 5.5) from $K_{3\pi D}$ events. The reconstructed invariant mass of $\pi^{\pm}\pi^0 e^+e^-$ candidates is shown in fig. 1. The normalization mode ($K_{2\pi D}$) is recorded concurrently with the signal mode, using the same trigger logic. A common event reconstruction is considered as much as possible aiming to cancel of systematic effects such as particle identification and trigger inefficiencies. The selection of the normalization mode $K_{2\pi D}$ uses the same set of requirements as the signal selection except for the π^0-reconstruction and background suppression parts. The neutral pion is reconstructed by requiring only one γ-candidate cluster and computing its invariant mass with the electron and positron pair. The only background source for the normalization channel is the $K_{\mu 3D}$ mode ($K^{\pm} \to \mu^+\nu\pi^0_D$). In the whole 2003 data sample 6.715 million $K_{2\pi D}$ candidates are selected with a background contamination smaller than 0.1%.

2˙2. *Branching ratio measurement*. – The total Branching Ratio of $K^{\pm} \to \pi^{\pm}\pi^0 e^+e^-$ is obtained using the expression

$$\mathcal{B}(K^{\pm} \to \pi^{\pm}\pi^0 e^+e^-) = \frac{N_S - N_B}{N_N}\frac{A_N\epsilon_N}{A_S\epsilon_S}\mathcal{B}(N), \tag{1}$$

where $N_{S,B,N}$ are the number of signal (1916), background (55.8 ± 7.4) and $K_{2\pi D}$ events. $A_{S,N}$ $\epsilon_{S,N}$ are the acceptances and trigger efficiencies of the signal and normalization modes. The normalization mode branching ratio $\mathcal{B}(N) = (2.425 \pm 0.076) \cdot 10^{-3}$ is obtained from the PDG [7] world average. The trigger efficiencies (ϵ), very similar ($\sim 98\%$) for signal and normalization mode, are measured on data using control sam-

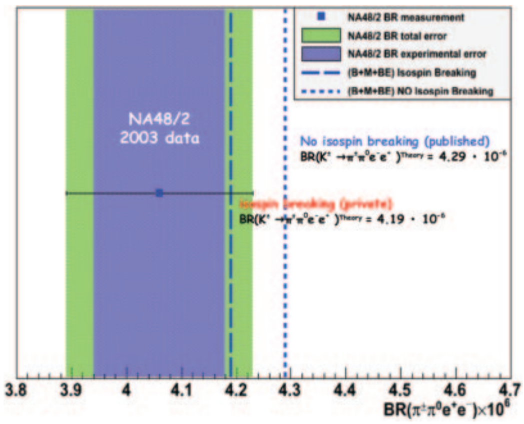

Fig. 2. – The $K^{\pm} \to \pi^{\pm}\pi^{0}e^{+}e^{-}$ preliminary branching ratio is plotted with its experimental error (shaded blue band) and its total error (shaded green band).

ples. The acceptances of the signal, the normalization and the background channels are computed using GEANT3-based [8] MC simulations which include the full detector and material description, stray magnetic fields, beam line geometry and local detector imperfections.

The MC simulation for the different $K^{\pm} \to \pi^{\pm}\pi^{0}e^{+}e^{-}$ contributions IB, DE, and the electric interference, have been generated separately according to the theoretical description given in [2] neglecting the magnetic interference in the present preliminary result. Due to limited statistic of the data sample the extraction of the DE and electric interference is not possible in this analysis. The signal acceptance has been obtained from a weighted average of the single components acceptances, using as weights the relative fractions computed in [2] on the basis of the measurement of magnetic and electric terms of $K^{\pm} \to \pi^{\pm}\pi^{0}\gamma$ in [6]:

$$A_S = \frac{A_{IB} + A_{DE} \cdot Frac_{DE} + A_{INT} \cdot Frac_{INT}}{1 + Frac_{DE} + Frac_{INT}}. \tag{2}$$

To take into account the E, M measurement uncertainties [6], the weights entering the total signal acceptance were varied accordingly resulting in a $\sim 1\%$ relative change quoted as the systematic uncertainty due to the acceptance modeling. As radiative corrections to the $K^{\pm} \to \pi^{\pm}\pi^{0}e^{+}e^{-}$ mode are not computed in [2], the NA48/2 signal MC simulation included the following effects: the classical Coulomb attraction/repulsion between charged particles and the real photon(s) emission as implemented in the PHOTOS package The preliminary result for the total branching ratio is obtained:

$$\mathcal{B}(K^{\pm} \to \pi^{\pm}\pi^{0}e^{+}e^{-}) = (4.06 \pm 0.10_{stat.} \pm 0.06_{syst.} \pm 0.13_{ext.}) \cdot 10^{-6}, \tag{3}$$

where systematic errors include uncertainties on acceptance, particle identification, trigger efficiencies and radiative corrections. The external error originating from the normalisation mode branching ratio uncertainty is the dominant error in the present measurement obtained with an overall precision of about 3%. The comparison with theoretical expectations is presented in fig. 2. The small dashed blue line represents the

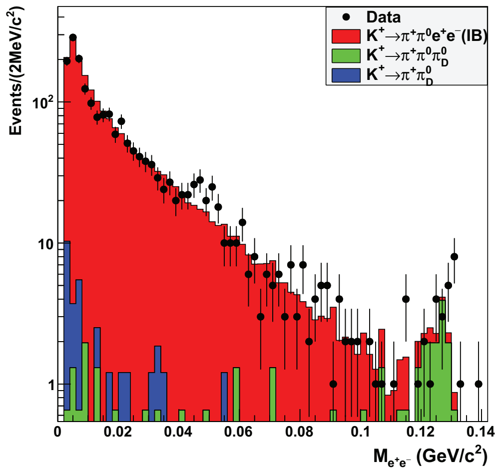

Fig. 3. – Reconstructed e^+e^- invariant mass distributions of the data and simulated background samples.

theoretical prediction with no isospin breaking correction published in [2]. The big dashed blue line shows the expected isospin breaking corrected branching ratio (private communication from the authors of [2]). The experimental value of the $\mathcal{B}(K^\pm \to \pi^\pm\pi^0 e^+e^-)$ is in a very good agreement with the theoretical predictions (within one standard deviation). The NA48/2 data sample analyzed has no sensitivity to the DE and INT contributions to the M_{ee} spectrum within the current statistics (see fig. 3). It will be difficult to perform a full Dalitz plot analysis without a proper description of the radiative effects, particularly relevant in a final state with two electron/positron.

3. – Search for the dark photon in π^0 decays

The large sample of π^0 mesons produced and decaying in vacuum collected by NA48/2 allows for a high sensitivity search for the dark photon (A'), a new gauge boson introduced in hidden sector new physics models with an extra $U(1)$ gauge symmetry. In a rather general set of models, the interaction of the dark photon (DP) with the ordinary matter is through kinetic mixing with the Standard Model hypercharge $U(1)$ [9]. In these models, the new coupling constant ε is proportional to the electric charge and the dark photon couples in exactly the same way to quarks and leptons. These scenarios could provide an explanation to the observed rise in the cosmic-ray positron fraction with energy, and could offer an explanation to the muon gyromagnetic ratio $(g-2)$ anomaly [10]. The simplest DP model is characterised by two free parameters, the DP mass $m_{A'}$ and the mixing parameter with the standard model ε. Its possible production in the π^0 decay and subsequent decay proceed via the following chain: $K^\pm \to \pi^\pm\pi^0$, $\pi^0 \to \gamma A'$, $A' \to e^+e^-$, producing a final state with three charged particles and a photon. The expected branching fraction of the π^0 decay is [11]

$$\mathcal{B}(\pi^0 \to \gamma A') = 2\varepsilon^2 \left(1 - \frac{m_{A'}^2}{m_{\pi^0}^2}\right)^3 \mathcal{B}(\pi^0 \to \gamma\gamma), \tag{4}$$

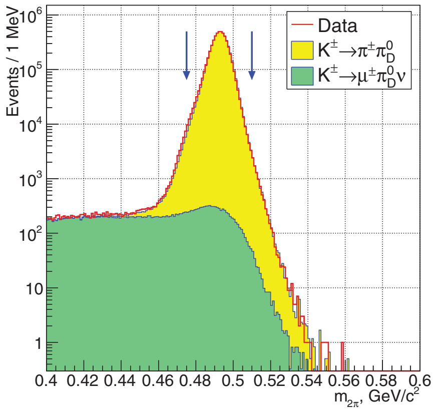

Fig. 4. – Reconstructed $\pi^{\pm}\pi^0_D$ invariant mass ($m_{2\pi}$) distributions of the data and simulated background samples. The selection condition is illustrated with arrows.

with a strong kinematic suppression of the decay rate for DP masses approaching m_{π^0}. In the mass range $2m_e \ll m_{A'} < m_{\pi^0}$ accessible in this analysis, assuming that the DP can only decay into SM fermions, $\mathcal{B}(A' \to e^+e^-) \approx 1$ while the allowed loop-induced decays ($A' \to 3\gamma$, $A' \to \nu\bar{\nu}$) are highly suppressed. The maximum DP mean path [11] in the NA48/2 experiment corresponds to an energy of approximately $E_{\max} = 50\,\text{GeV}$:

$$L_{\max} \approx (E_{\max}/m_{A'})c\tau \approx 0.4\,\text{mm} \times \left(\frac{10^{-6}}{\varepsilon^2}\right) \times \left(\frac{100\,\text{MeV}}{m_{A'}}\right)^2 .$$

In the accessible parameter range ($m_{A'} > 10\,\text{MeV}/c^2$ and $\varepsilon^2 > 5 \times 10^{-7}$) $L_{\max}$ does not exceed 10 cm and the DP can be assumed to decay at the production point. In this prompt decay scenario the NA48/2 3-track vertex reconstruction does not introduce significant acceptance losses as the typical resolution on the vertex longitudinal coordinate is ≈ 1 m. The DP signature is identical to that of the Dalitz decay $\pi^0_D \to e^+e^-\gamma$, which therefore represents an irreducible background and limits the sensitivity. The largest π^0_D sample, and therefore the largest sensitivity, is obtained form the study of the $K^{\pm} \to \pi^{\pm}\pi^0_D$ decays.

3·1. *Event selection and background simulation.* – The full NA48/2 data sample is used for the analysis. The $K_{2\pi D}$ event selection requires a three-track vertex reconstructed in the fiducial decay region formed of a pion ($\pi^{\pm}$) candidate track and two opposite-sign electron ($e^{\pm}$) candidate tracks. Charged particle identification is based on the ratio of energy deposition in the LKr calorimeter to the momentum measured by the spectrometer, which should be smaller (greater) than 0.85 for pion (electron) candidates. Furthermore, a single isolated LKr energy deposition cluster is required as the photon candidate. The reconstructed invariant mass of the $\pi^{\pm}\pi^0$ system (fig. 4) is required to the consistent with the $K^{\pm}$ mass. A sample of 4.687×10^6 fully reconstructed π^0_D decay candidates in the e^+e^- invariant mass range $m_{ee} > 10\,\text{MeV}/c^2$ with a negligible background is selected. The candidates mainly originate from $K_{2\pi D}$ decays, with 0.15% coming from the semileptonic $K^{\pm} \to \pi^0_D\mu^{\pm}\nu$ decays (denoted $K_{\mu 3D}$ below). Correcting the observed number of candidates for acceptance and trigger efficiency, the total number

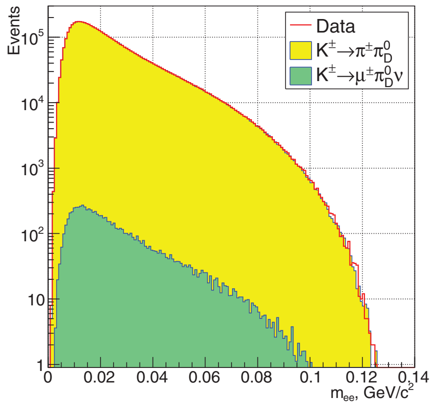

Fig. 5. – Reconstructed e^+e^- invariant mass distributions of the data and simulated $K_{2\pi D}$ and $K_{\mu 3D}$ samples.

of $K^\pm$ decays in the 98 m long fiducial decay region for the analyzed data sample is found to be $N_K = (1.55 \pm 0.05) \times 10^{11}$, where the quoted error is dominated by the external uncertainty on the π^0_D decay branching fraction $\mathcal{B}(\pi^0_D)$. The reconstructed e^+e^- invariant mass (m_{ee}) spectrum of the $K_{2\pi D}$ candidates is displayed in fig. 5. A dark photon produced in the π^0_D decay and decaying promptly to e^+e^- would appear as narrow peak in the spectrum. Monte Carlo (MC) simulations of the $K_{2\pi D}$ and $K_{\mu 3\mathrm{D}}$ processes are performed to subtract the irreducible π^0_D background. The π^0_D decay is simulated using the lowest-order differential decay rate in [12]. Radiative corrections to the differential rate are implemented following the approach of Mikaelian and Smith [12] recently revised to improve the numerical precision [13]. The method introduces only weights $\delta(x, y)$ and does not account for the emission of inner bremsstrahlung photons.

3˙2. *Dark photon search technique*. – A search for the DP is performed assuming different mass hypotheses with a variable mass step. The mass step of the scan and the width of the signal mass window around the assumed DP mass are determined by the resolution on the e^+e^- invariant mass. The mass step of the DP scan is set to be $\sigma_m/2$, while the signal region mass window for each DP mass hypothesis is defined as $\pm 1.5\sigma_m$ around the assumed mass (both the scan step and the mass window half-width are rounded to the nearest multiple of $0.02\,\mathrm{MeV}/c^2$). The mass window width has been optimised with MC simulations to obtain the highest sensitivity to the DP signal, determined by a trade-off between π^0_D background fluctuation and signal acceptance.

In total, 398 DP mass hypotheses are tested in the range $10\,\mathrm{MeV}/c^2 \leq m_{ee} < 125\,\mathrm{MeV}/c^2$. The lower limit of the considered mass range is determined by the limited precision of MC simulation of background at low mass, while at the upper limit of the mass range the signal acceptance drops to zero. The numbers of observed data events in the signal region (N_{obs}) and the numbers of π^0_D background events expected from MC simulation corrected by the measured trigger efficiencies (N_{exp}) in the DP signal window for each considered mass hypothesis are presented in fig. 6. They decrease with the DP mass due to the steeply falling π^0_D differential decay rate and decreasing acceptance, even though the mass window width increases, being approximately proportional to the mass.

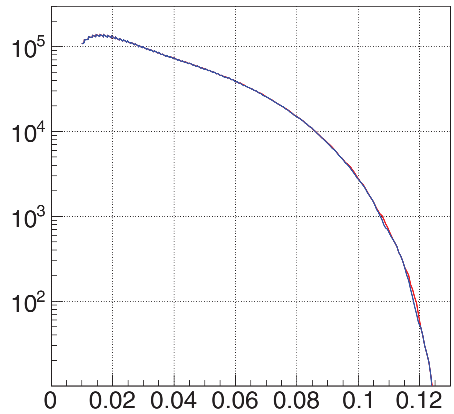

Fig. 6. – Numbers of observed (red) and expected (blue) DP candidates in the DP signal mass window as for each assumed DP mass hypothesis.

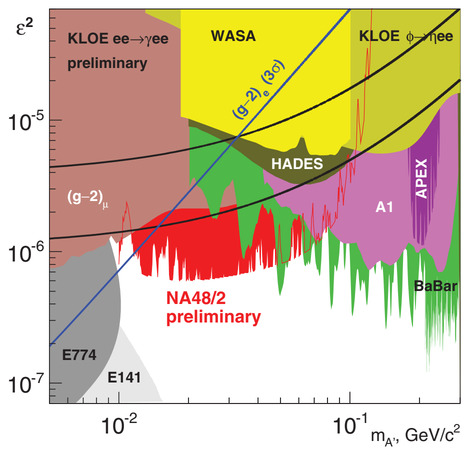

Fig. 7. – The NA48/2 preliminary upper limits at 90% CL on the mixing parameter ε^2 *vs.* the DP mass $m_{A'}$, compared to the other published exclusion limits.

Confidence intervals at 90% CL for the number of $A' \to e^+e^-$ decay candidates ($N_{\rm DP}$) in each mass hypothesis ($N_{\rm DP}$) are available from $N_{\rm obs}$, $N_{\rm exp}$ and $\delta N_{\rm exp}$ using the Rolke-López method [14] assuming Poissonian (Gaussian) errors on the numbers of observed (expected) events. For the preliminary results, it is assumed conservatively that $N_{\rm obs} = N_{\rm exp}$ in cases when $N_{\rm obs} < N_{\rm exp}$, as the employed implementation of the method (from the ROOT package) has been found to underestimate the upper limits in that case. Upper limits at 90% CL on $\mathcal{B}(\pi^0 \to \gamma A')$ in each DP mass hypothesis in the assumption $\mathcal{B}(A' \to e^+e^-) = 1$ are computed using the relation

$$\mathcal{B}(\pi^0 \to \gamma A') = \frac{N_{\rm DP}}{N_K}\Big[\mathcal{B}(K_{2\pi})A(K_{2\pi}) + \mathcal{B}(K_{\mu 3})A(K_{\mu 3})\Big]^{-1}.$$

The acceptances $A(K_{2\pi})$ and $A(K_{\mu 3})$ of the employed $K_{2\pi D}$ event selection for the $K_{2\pi}$ and $K_{\mu 3}$ decays, respectively, followed by the prompt $\pi^0 \to \gamma A'$, $A' \to e^+e^-$ decay chain, are evaluated for each considered DP mass with MC simulation. Event distributions in the angle between e^+ momentum in the e^+e^- rest frame and the e^+e^- momentum in the π^0 rest frame are identical for the decay chain involving the DP ($\pi^0 \to \gamma A'$, $A' \to e^+e^-$) and the π^0_D decay, up to a negligible effect of the radiative corrections that should not be applied in the former case. Therefore DP acceptances are evaluated using the MC samples produced for background description.

The largest uncertainty on the computed $\mathcal{B}(\pi^0 \to \gamma A')$ is the external one due to $\mathcal{B}(\pi^0)$ entering via N_K. It amounts to 3% in relative terms and is neglected. The obtained upper limits on $\mathcal{B}(\pi^0 \to \gamma A')$ are $\mathcal{O}(10^{-6})$ and do not exhibit a strong dependence on the assumed DP mass, as the negative trends in background fluctuation (fig. 6) and acceptance largely cancel out. Upper limits at 90% CL on the mixing parameter ε^2 in each considered DP mass hypothesis are calculated from those on $\mathcal{B}(\pi^0 \to \gamma A')$ using eq. (4). The resulting preliminary DP exclusion limits, along with constraints from other experiments [15], the band of phase space where the discrepancy between the measured and calculated muon $g-2$ values falls into the $\pm 2\sigma$ range [10, 16] due to the DP contribution, and the region excluded by the electron $g-2$ measurement, are presented in fig. 7. The obtained upper limits on ε^2 represent an improvement over the existing data in the DP mass range 10–60 MeV/c^2. Under the assumption that the DP couples to SM through kinetic mixing and decays predominantly to SM particles, the NA48/2 preliminary result excludes the DP as an explanation for the muon $(g-2)$ anomaly in the range 10–100 MeV/c^2.

REFERENCES

[1] Fanti V. *et al.*, *Nucl. Instrum. Methods A*, **574** (2007) 443.
[2] Cappiello L., Cata O., D'Ambrosio G. and Gao D. N., *Eur. Phys. J. C*, **72** (2012) 1872.
[3] Christ N., *Phys. Rev.*, **159** (1967) 1292.
[4] Pichl H., *Eur. Phys. J. C*, **20** (2001) 371.
[5] Gevorkyan S. R. and Misheva M. H., *Eur. Phys. J. C*, **74** (2014) 2860.
[6] Batley J. R. *et al.* [NA48/2 Collaboration], *Eur. Phys. J. C*, **68** (2010) 75.
[7] Olive K. A. *et al.* (Particle Data Group), *Chin. Phys. C*, **38** (2014) 090001.
[8] GEANT Detector Description and Simulation Tool, CERN Program Library W5013 1994.
[9] Holdom B., *Phys. Lett. B*, **166** (1986) 196.
[10] Pospelov M., *Phys. Rev. D*, **80** (2009) 095002.
[11] Batell B., Pospelov M. and Ritz A., *Phys. Rev. D*, **80** (2009) 095024.
[12] Mikaelian K. O. and Smith J., *Phys. Rev. D*, **5** (1972) 1763.
[13] Husek T., Kampf K. and Novotny J., *Phys. Rev. D*, **92** (2015) 054027.
[14] Rolke W. A. and López A. M., *Nucl. Instrum. Methods A*, **458** (2001) 745.
[15] Lees J. P. *et al.*, *Phys. Rev. Lett.*, **113** (2014) 201801 and references therein.
[16] Davoudiasl H., Lee H.-S. and Marciano W. J., *Phys. Rev. D*, **89** (2014) 095006.